

THE PIONIC SODIUM  $2p$ - $1s$  TRANSITION

D.I. BRITTON, G.A. BEER, J.A. MACDONALD, G.R. MASON, T. NUMAO,  
A. OLIN and P.R. POPFENBERGER.

University of Victoria, Victoria, B.C., Canada,  
and TRIUMF, Vancouver, B.C., Canada

A.R. KUNSELMAN

University of Wyoming, Laramie, WY, USA

B.H. OLANTYI

University of Ife, Ile-Ife, Nigeria

Abstract

The width and energy of the pionic sodium  $2p$ - $1s$  X-ray has been measured using a Compton suppressed germanium spectrometer. The resulting reduction of the continuum Compton background has allowed a more detailed determination of the X-ray. The values obtained are: Energy =  $276.45(\pm 0.27, \pm 0.33)$  keV; Width =  $17.1(\pm 1.1, \pm 1.2)$  keV. The measured width is in better agreement with optical model predictions than previous measurements which gave anomalously narrow values.

(Submitted to Nuclear Physics A)



1. Introduction

The energy levels of pionic atoms are determined primarily by the electromagnetic interaction, but the lower levels are broadened by pion absorption and shifted due to multiple scattering by the nucleons in the nucleus. The optical potentials, developed in a phenomenological manner to describe these strong interaction effects, produce results that are generally in good agreement with experiment over a wide range of mass numbers. These potentials also give a good account of low energy pion scattering data, where the negative pion data are particularly sensitive to the neutron matter distribution in the nucleus.

With increasing  $Z$ , the absorptive broadening of a particular level becomes more severe and the transition intensity to the broadened level decreases as absorption from the feeding level increases. Consequently, there arises a weakest observable X-ray transition to each of the  $s$ ,  $p$ ,  $d$  and  $f$  levels and in each case measurements of these weak transitions have yielded anomalous strong interaction widths and shifts<sup>5</sup>). In particular, measured values of the  $\pi$ Na  $2p$ - $1s$  X-ray width range between 4.6 and 12.0 keV (see Table 1), whereas optical model calculations predict values in the range 17-22 keV<sup>1,6</sup>). In an attempt to resolve this discrepancy, a new measurement was made at TRIUMF using a Compton suppression spectrometer to reduce the Compton continuum in the region of the X-ray.

2. Experimental method

The experiment was performed using a 90 MeV/c negative pion beam from the TRIUMF M13 channel in the setup illustrated in fig. 1. The pions were degraded in 1 cm of beryllium and stops in the NaH target were defined by a conventional four-scintillator telescope (S1 to S4). The disc-shaped NaH target (1.0 cm thick by 6.3 cm diameter), contained in

1 K 1 1 1 06-6  
C2

TRI-PP-86-6  
Feb 1986

BB  
CERN LIBRARY  
02 JUN 1986

**THE PIONIC SODIUM 2p-1s TRANSITION**

D.I. BRITTON, G.A. BEER, J.A. MACDONALD, G.R. MASON, T. NUMAO,  
A. OLIN and P.R. POFFENBERGER.

University of Victoria, Victoria, B.C., Canada,  
and TRIUMF, Vancouver, B.C., Canada

A.R. KUNSELMAN

University of Wyoming, Laramie, WY, USA

B.H. OLANIYI

University of Ife, Ile-Ife, Nigeria

**1. Introduction**

The energy levels of pionic atoms are determined primarily by the electromagnetic interaction, but the lower levels are broadened by pion absorption and shifted due to multiple scattering by the nucleons in the nucleus. The optical potentials, developed in a phenomenological manner to describe these strong interaction effects, produce results that are generally in good agreement with experiment over a wide range of mass numbers. These potentials also give a good account of low energy pion scattering data, where the negative pion data are particularly sensitive to the neutron matter distribution in the nucleus.

With increasing Z, the absorptive broadening of a particular level becomes more severe and the transition intensity to the broadened level decreases as absorption from the feeding level increases. Consequently, there arises a weakest observable X-ray transition to each of the s, p, d and f levels and in each case measurements of these weak transitions have yielded anomalous strong interaction widths and shifts<sup>6</sup>. In particular, measured values of the  $\pi$ Na 2p-1s X-ray width range between 4.6 and 12.0 keV (see Table 1), whereas optical model calculations predict values in the range 17-22 keV<sup>1,6</sup>. In an attempt to resolve this discrepancy, a new measurement was made at TRIUMF using a Compton suppression spectrometer to reduce the Compton continuum in the region of the X-ray.

**2. Experimental method**

The experiment was performed using a 90 MeV/c negative pion beam from the TRIUMF M13 channel in the setup illustrated in fig. 1. The pions were degraded in 1 cm of beryllium and stops in the NaH target were defined by a conventional four-scintillator telescope (S1 to S4). The disc-shaped NaH target (1.0 cm thick by 6.3 cm diameter), contained in

**Abstract**

The width and energy of the pionic sodium 2p-1s X-ray has been measured using a Compton suppressed germanium spectrometer. The resulting reduction of the continuum Compton background has allowed a more detailed determination of the X-ray. The values obtained are: Energy = 276.45( $\pm 0.27$ ,  $\pm 0.33$ ) keV; Width = 17.1( $\pm 1.1$ ,  $\pm 1.2$ ) keV. The measured width is in better agreement with optical model predictions than previous measurements which gave anomalously narrow values.

(Submitted to Nuclear Physics A)



011 200007400

thin polystyrene, was mounted at  $45^\circ$  to the beam axis to reduce attenuation of X-rays before they entered the detector, which was positioned at  $90^\circ$  to the beam. The target was made thin and of low-density NaH (rather than sodium metal) in order to reduce the intensity of the  $\text{Na}(n,n')$  440 keV gamma-ray, which has a Compton edge at the same energy as the  $\pi\text{Na}$  2p-1s X-ray. The detector was p-type coaxial intrinsic germanium with 1.0 keV resolution in the region of the broadened X-ray (276 keV). It was positioned 36 cm from the target, allowing time-of-flight separation of gamma-rays from neutrons up to 30 MeV. This corresponded to a timing resolution of 4 ns FWHM at 1.3 MeV, and effectively removed the  $\text{Ge}(n,n')\gamma$  background.

The detector was surrounded by a compact bismuth germanate (BGO) Compton suppression system<sup>2</sup>). This was of a segmented design comprising sixteen  $80 \times 55 \times 55$  mm BGO crystals to allow high rate capability. The system improved the photopeak to Compton background ratio by a factor of 5. The use of bismuth germanate, rather than  $\text{NaI}(\text{Tl})^3$ , was essential in the present experiment because a  $\text{NaI}(\text{Tl})$  system would have introduced many more counts into the Compton edge of the neutron-induced sodium 440 keV gamma-ray. The detection system was collimated and shielded from the target with lead, copper, and tungsten plates and with borated gypsum bricks to moderate and capture neutrons. The up-stream side of the suppressor was also well shielded with lead to reduce false vetoes.

The slow linear signal from the germanium detector was digitized by an ADC that was bias- and gain-stabilized on two known peaks in the prompt spectrum ( $\pi\text{Cl}$  3d-2p at 150.56 keV and a  $^{137}\text{Cs}$  gamma at 661.66 keV). For each event, the energy and its time relative to the pion stop were recorded on magnetic tape. For some runs, the Compton

veto was not included in the trigger, but was used to set a bit in a pattern register; recording these data allowed evaluation of the suppressor under in-beam conditions<sup>2</sup>). In addition, a stop in the degrader was used to provide a beam-rate dependent random trigger for events consisting of longer lived gamma-rays induced by pion capture or of gamma-rays from an adjacent  $^{137}\text{Cs}$  source. They were used to provide information for calibration and on the detector response function under in-beam conditions. To determine detector efficiency throughout the X-ray region, spectra from  $^{75}\text{Se}$  and  $^{133}\text{Ba}$  sources were recorded. The spectrum from an activated gold source, with a gamma-ray at 412 keV, was recorded to facilitate fitting the  $\text{Na}(n,n')$  Compton edge of the 440 keV gamma-ray.

### 3. Data analysis

The energy spectra were analyzed using a  $\chi^2$  minimization routine<sup>4</sup>). The fitting function consisted of a Gaussian line shape with a low energy, two-parameter exponential tail. To describe the absorptive broadening of the X-ray, this line shape was convoluted with a Lorentzian distribution that had been corrected for changes in detector efficiency with energy. The peaks were fitted on a linear background since the effect of including an exponential term was shown to be within the uncertainty of the linear background. The possibility of a step-like background under the peaks was assessed and included in the systematic uncertainty. Such a step-shaped background has been conjectured to arise from a uniform excess of counts on the low energy side of a peak due to charge loss in the detector. In contrast, pileup can produce an excess of counts on the high energy side and the limit on the net step, determined from the in-beam spectra, was 0.2%/keV of the peak area.

Energy calibration was determined from well known X-rays and gamma-rays produced by stops in the target and from the in-beam source data acquired in coincidence with a stop in the degrader; these calibration peaks are listed in table 2. The energies of the gamma-rays versus the peak channel numbers were fitted to both a linear and a quadratic function using a least-squares fit in order to estimate the effect of nonlinearities in the energy determination. The quadratic term was negligible, being of the order  $10^{-8}$ . The Compton edge of the  $\text{Na}(n, n')$  440 keV gamma-ray was fitted with suitably scaled fits to the Compton edge of the 412 keV gamma-ray from the Au source: The Compton suppressor had the effect of transforming the edge into a broad peak corresponding to lost photons which scattered back out of the entrance hole of the suppressor at  $180^\circ$ . Therefore, the gold Compton edge was fitted as a Lorentzian broadened peak which was then scaled in position and intensity to approximate the sodium Compton edge. The entire effect of adding the Compton edge was included as part of the systematic uncertainty, with a contribution of  $\pm 0.07$  keV in the energy and  $\pm 0.07$  keV in the width. This is an improvement over previous measurements where the problem was one of fitting the unsuppressed Compton edge. In addition, since the 440 keV gamma-ray is produced by secondary reactions in the target, the use of a thin low density target further reduced the intensity of this line as compared with previous measurements.

One of the most important factors in determining the width of the X-ray was establishing the background. A large energy region extending from 215 keV to 335 keV was fitted. This region was limited on the lower side by the Compton edge of the 350 keV  $^{21}\text{Ne}$  gamma-ray at 202 keV, and on the upper side by the low energy tail of the 350 keV gamma-ray itself.

The  $\pi\text{Na } 3p\text{-}1s$  X-ray at 339 keV, calculated to be 8.5% of the  $\pi\text{Na } 2p\text{-}1s$  intensity by an X-ray cascade code<sup>5</sup>, was included in the fit.

Fig. 2 shows the main structures in the fitted region as well as the final fit. The large peak at 250 keV is the  $\mu\text{Na}(2\text{-}1)$  X-ray, and the large peak at 300 keV is a superposition of the  $\mu\text{Na}(3\text{-}1)$  X-ray and a  $^{16}\text{N}^*$  gamma-ray. These peaks and the region immediately below the 250 keV peak were poorly described by the fitting function. Since they contain minimal information about the broad X-ray and their contribution to the fit was dominated by their statistical uncertainty, they were not included in the final fit.

Closer examination of the three well-defined and identified contaminant gamma-rays at the centroid of the X-ray suggested the possibility of two further gammas as shown in the insert in fig. 2. When these were included in the fit, the fitted width of the broad X-ray increased by 2 keV accompanied by a marginal improvement in  $\chi^2$  (Total  $\chi^2$  changing from 751 to 736). Since there is only weak evidence for the existence of these extra peaks, their effect on the X-ray's width is included as the dominant contribution to the systematic uncertainty and the final result was centered in the uncertainty range. Other contributions to the uncertainties are listed in table 3.

#### 4. Results and discussion

The theoretical width and shift obtained for the sodium pionic  $2p\text{-}1s$  X-ray depends on the particular optical potential and parameters used. Poffenberger<sup>1</sup>) performed a global fit of the best pionic X-ray data from light nuclei, and in an attempt to extend this fit to describe the anomalously narrow experimental width for sodium he investigated the large dependence of the sodium width and shift on the neutron

distribution. He concluded that the theoretical width goes through a minimum of about 17 keV as the neutron distribution is varied.

Batty, Friedman and Gal<sup>6</sup>) performed an analysis where they examined whether anomalies such as that for sodium, set in gradually or abruptly, and attempted to remove these so called saturation phenomena by using several modifications to the optical potential. The conclusions of their analysis, which illustrate the impetus behind the present work, are that no reasonable modification of the optical potential could explain the anomalous results, and that the transition from normal to anomalous experimental result is abrupt with respect to atomic number. In the case of the 1s level this is shown by a good fit to <sup>20</sup>Ne, but a poor fit to <sup>23</sup>Na. Thus the anomaly is due either to a new and unknown effect that sets in suddenly, or to experimental problems.

The result of the present analysis of the sodium X-ray is presented in table 1, along with the other published results, and the theoretical values of Poffenberger<sup>1</sup>) and Batty et al.<sup>6</sup>). The measured energy is 276.45(±0.27,±0.33) keV and the measured width is 17.1(±1.1,1.2) keV where the first quoted uncertainty is statistical and the second is the sum in quadrature of the systematic uncertainties. It can be seen from table 1 that this experimental width is significantly larger than the previously determined widths, including that obtained by a group at TRIUMF in 1978 working without a Compton suppressor. However, when the Compton suppressed data is fitted over the same energy region, and with the same contaminant peaks as fitted in the previous data set, a result consistent with the 1978 result is obtained. The earlier analysis<sup>7-9</sup>) were unable to distinguish now prominent contaminant gamma-rays on top the X-ray, which caused them to underestimate the absorptive width. We

conclude that the uncertainties were seriously underestimated in previous work. The present result is consistent with some optical model predictions, but it can also accommodate a 30% reduction from the predicted absorption width.

#### Acknowledgements

This research was supported by grants from the Natural Sciences and Engineering Research Council of Canada. It is also a pleasure to acknowledge assistance during the preparation and running of this experiment by G.M. Marshall, J.W. Forsman and P. van Esbroek.

References

- 1) P.R. Poffenberger, Ph.D. Dissertation, University of Victoria, 1981.
- 2) A. Olin, P.R. Poffenberger and D.I. Britton, Nucl. Instr. Meth. **222** (1984) 463.
- 3) R. Beetz, W.L. Posthumus, F.W.N. De Boer, J.L. Maarleveld, A. van der Schaaf, and J. Konijn, Nucl. Instr. Meth. **145** (1977) 353.
- 4) A. Olin, "Jagspot: A Code For Fitting Complex Gamma Ray Spectra", University of Victoria TRIUMF Report VPN-78-2.
- 5) M. Krell, The pionic atom program: PIATOM, University of Victoria, TRIUMF Report VPN-77-5.
- 6) C.J. Batty, E. Friedman and A. Gal, Nucl. Phys. **A402** (1983) 411.
- 7) G. Backenstoss, S. Charalambus, H. Daniel, H. Koch, G. Poelz, H. Schmitt and L. Tauscher, Phys. Lett. **25B** (1967) 365.
- 8) D. Jenkins, R. Kunselman, M.K. Simmons and T. Yamazaki, Phys. Rev. Lett. **17** (1966) 1.
- 9) G.H. Miller, M. Eckhause, W.W. Sapp and R.E. Welsh, Phys. Lett. **27B** (1968) 663.
- 10) A. Olin, G. Beer, D. Bryman, M. Dixit, J. Macdonald, G. Mason, R. Pearce and P. Poffenberger, Nucl. Phys. **A312** (1978) 361.
- 11) I. Schwanner, G. Backenstoss, W. Kowald, L. Tauscher, H.J. Weyer, D. Gotta and H. Ullrich, Nucl. Phys. **A412** (1984) 253.
- 12) R.J. DeWitjer, H.S. Plendl and R. Holub, Atomic Data and Nuclear Data Tables **13** (1974) 1.
- 13) L.A. Schaner, T. Dubler, K. Kaeser, G.A. Rinker, Jr., B. Robert-Tissot, L. Scheellenberg and H. Schneuwly, Nucl. Phys. **A300** (1974) 225.
- 14) C.M. Lederer et al., Table of Isotopes, 7th ed., John Wiley (1978) App. 4.

Table 1.

Results for the Energy, Widths and Shifts of the Pionic 2-1 X-ray in Sodium (in units of keV).

Experimental:	Energy	Shift	Width
Backenstoss et al. <sup>7)</sup>	276.2(1.0)	-51.0	10.3(4.0)
Jenkins et al. <sup>8)</sup>	277.2(1.0)	-50.0	4.6(3.0)
Miller et al. <sup>9)</sup>	277.5(0.5)	-49.7	6.2(1.2)
Olin et al. <sup>10)</sup>	275.75(0.26)	-51.4	12.0(1.2)
Current Work	276.45 (±0.33syst)	-50.7	17.1 (±1.1stat) (±1.2syst)
Theoretical:	Energy	Shift	Width
Poffenberger <sup>1)</sup>	(R <sub>n</sub> =2.98 fm) 276.16	-51.04	17.62
Batty et al. <sup>6)</sup>	(R <sub>n</sub> =2.96 fm) 278.61	-48.6	21.98

Table 2

The calibration peaks

Peak	Peak Channel	Energy in keV
$\pi$ -Cl (3-2)	1045.9 (0.1)	150.560(0.035) <sup>11)</sup>
<sup>19</sup> F-gamma	1370.76 (0.06)	197.15 (0.01) <sup>12)</sup>
$\mu$ -Na (2-1)	1740.75 (0.10)	250.256(0.033) <sup>13)</sup>
<sup>21</sup> F-gamma	1947.8 (0.2)	279.92 (0.06) <sup>12)</sup>
<sup>137</sup> Cs-gamma	4611.37 (0.05)	661.661(0.003) <sup>14)</sup>

Table 3

Contributions to the Uncertainties in Pionic Sodium

	Energy (keV)	Width (keV)
Contaminants	0.18	1.00
Background	0.07	0.34
Resolution	0.04	0.57
Tailing/Step Background	0.25	0.29
Compton edge (Na(n,n') at 440 keV)	0.07	0.07
Efficiency	0.03	0.04
Calibration	0.01	0.00
Total systematic uncertainty	0.33	1.24
Statistical uncertainty	0.27	1.10

Figure captions

1. Schematic of the experimental layout.
2. X-ray spectrum showing the regions fitted. The insert is a detail of the central region showing the  $\gamma$ -rays considered in the fit (See text).

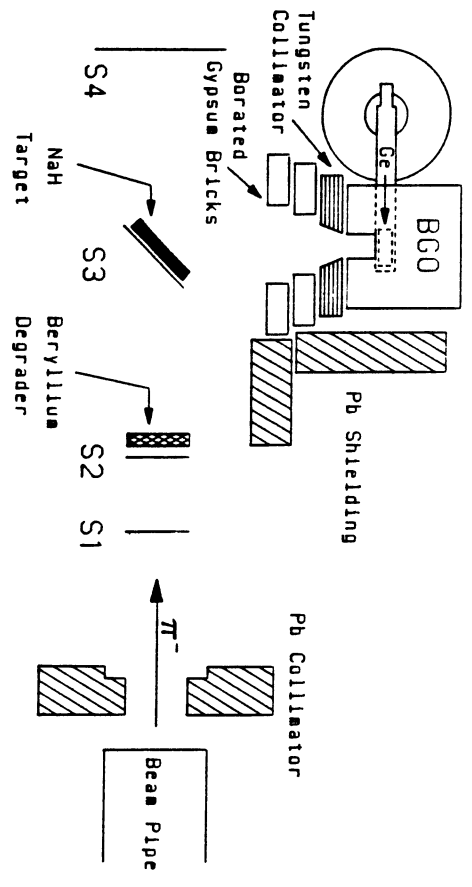


Fig. 1

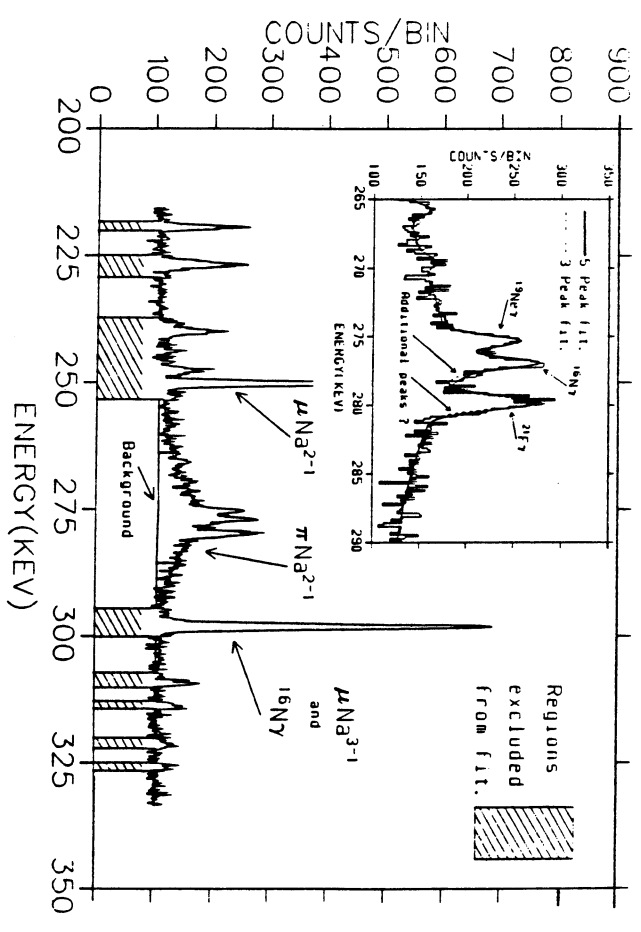


Fig. 2